Validation of the dynamic wake meander model with focus on tower loads

Larsen, Torben J.; Larsen, Gunner Chr.; Pedersen, Mads Mølgaard; Enevoldsen, Karen; Madsen, Helge Aagaard

Published in:
Wake Conference 2017

Link to article, DOI:
10.1088/1742-6596/854/1/012027

Publication date:
2017

Document Version
Publisher's PDF, also known as Version of record

Validation of the Dynamic Wake Meander model with focus on tower loads

2017 J. Phys.: Conf. Ser. 854 012027

(http://iopscience.iop.org/1742-6596/854/1/012027)

IOP Conf. Series: Journal of Physics: Conf. Series **854** (2017) 012027 doi:10.1088/1742-6596/854/1/012027

Validation of the Dynamic Wake Meander model with focus on tower loads

T.J. Larsen[1], G.C. Larsen[1], M.M. Pedersen[1], K. Enevoldsen[1], H.A. Madsen[1]

[1]Technical University of Denmark, Department of Wind Energy, tjul@dtu.dk

Abstract. This paper presents a comparison between measured and simulated tower loads for the Danish offshore wind farm Nysted 2. Previously, only limited full scale experimental data containing tower load measurements have been published, and in many cases the measurements include only a limited range of wind speeds. In general, tower loads in wake conditions are very challenging to predict correctly in simulations. The Nysted project offers an improved insight to this field as six wind turbines located in the Nysted II wind farm have been instrumented to measure tower top and tower bottom moments. All recorded structural data have been organized in a database, which in addition contains relevant wind turbine SCADA data as well as relevant meteorological data – e.g. wind speed and wind direction – from an offshore mast located in the immediate vicinity of the wind farm. The database contains data from a period extending over a time span of more than 3 years. Based on the recorded data basic mechanisms driving the increased loading experienced by wind turbines operating in offshore wind farm conditions have been identified, characterized and modeled. The modeling is based on the Dynamic Wake Meandering (DWM) approach in combination with the state-of-the-art aeroelastic model HAWC2, and has previously as well as in this study shown good agreement with the measurements. The conclusions from the study have several parts. In general the tower bending and yaw loads show a good agreement between measurements and simulations. However, there are situations that are still difficult to match. One is tower loads of single-wake operation near rated ambient wind speed for single wake situations for spacing's around 7-8D. A specific target of the study was to investigate whether the largest tower fatigue loads are associated with a certain downstream distance. This has been identified in both simulations and measurements, though a rather flat optimum is seen in the measurements.

1. Introduction

Fatigue loads on wind turbines are mainly driven by the varying inflow condition, where especially turbulence and shear are the most dominating contributors. Especially for offshore turbines, the ambient turbulence levels are typically small with average turbulence intensity around 6%. As offshore turbines are typically placed in wind farms, the turbulence driven fatigue contribution is, depending on the wind farm layout, dominated by wake effects of the neighboring wind turbines. It is therefore important to be able to model these effects with high accuracy to ensure the right load level and to be able to utilize new advanced passive or active load reducing strategies to alleviate the wake induced loading. Usually these effects are included in simulations using the method from Frandsen [1],[2], which basically adjust the turbulence level based on the distance to the nearest wind turbine. This may be a sufficient method for many applications and site evaluations, especially when the turbine spacing is close to 8 diameters (D), which was the distance the model was originally derived

for. The method used in this paper is however based on the Dynamic Wake Meander (DWM) approach [3],[4],[5],[6] where the wake is modeled as a wind speed deficit that is transported from the upstream turbine in a meandering way prescribed by the large turbulence structures. This model has been validated based on full scale measurements in [5],[6]. An interesting consequence of the wake meandering approach is that for very short distances, the meandering is limited, but the deficit is large, i.e. the downwind turbine to have a low thrust and power production while the blade load variations are high in half-wake situations. The tower load variations are not expected to increase, as this is mainly sensitive to varying thrust of the full rotor – typically not seen at short distances (<3D). For very large spacing (>15D) the deficit is reduced to a degree where the load impact on the downstream turbine is minimal.
Consequently, the tower load level reach its maximum level between 3D and 15D, which is the typical spacing in most wind farms today. To see if this can be observed experimentally, the Nysted II experiment was setup with tower load measurement on several turbines with different spacing, so that a broad range of distances could be covered. The result of this study, together with at general load comparison, is presented in this paper.

2. Experimental setup

The Nysted II wind farm consist of 90 Siemens SWT2.3 PRVS turbines installed in the southern part of Denmark, see Figure 1. A total of 6 turbines were instrumented with strain gauges in top and bottom of the tower. The available measurements can be divided into 5 data classes, each with their own characteristics, data coverage and time stamp reference.

1) High frequency sampled meteorological data.
2) High frequency sampled WT structural strain-gauge data.
3) Time series data from WT Supervisory Control And Data Acquisition (SCADA) systems.
4) Statistical 10-minute meteorological data.
5) Statistical data from the WT SCADA systems.

The high frequency sampled (i.e. 20 Hz) meteorological data consist of recordings from 3 Sonics mounted on an off-shore meteorological mast nearby the WF in altitudes 17m, 40m and 57m above mean sea level (AMSL), respectively. The high sampled (i.e. 40 Hz) structural data consist of strain-gauge measurements from the 6 instrumented turbines (L1, L2, L3, M1, M2, K18) – cf. Figure 1. For each WT, the strain-gauge setup resolves two WT tower bottom bending moments and two WT tower top bending moments in mutual perpendicular directions as well as the tower top torsion (i.e. yaw) moment. It was however problematic to use the tower top bending moment as local stress concentrations affecting the strain gauges removed the usable signal from several sectors. The analyses in this paper are therefore based on the tower bottom bending moment and the tower top yaw moment.

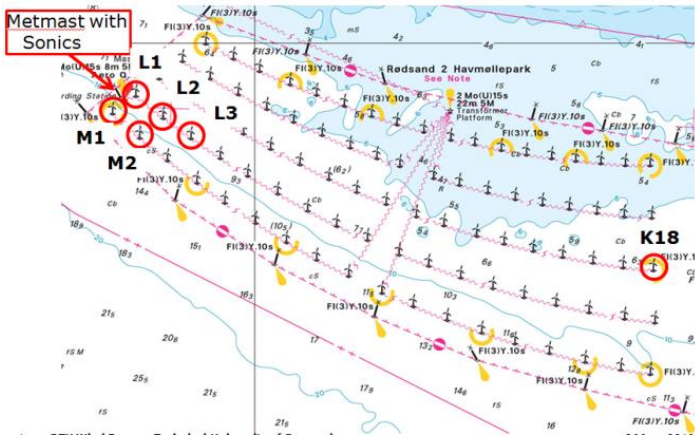

Figure 1 Site overview with instrumented WTs indicated.

3. Turbine and ambient inflow conditions

The baseline is a model of a 2.3MW pitch regulated turbine equipped with the DTU controller [14] in order to mimic as close as possible the Siemens 2.3MW WTs at the Nysted II site. Simulations have been performed for mean wind speeds ranging between 6m/s and 24m/s with increments of 2m/s. The ambient turbulence level has been chosen to 6%, corresponding approximately to the mean turbulence level at different previously investigated offshore WFs (Egmond aan Zee, Lillgrund, Horns Rev I) as well as to the mean of the undisturbed ambient turbulence intensity level at the present Nysted II site. In Figure 3 the measured turbulence intensity has been given for the full polar (i.e. [0^o; 360^o]), and as seen significant systematic variations are observed. These are partly caused by upstream (turbulence generating) WTs (i.e. L1, M1, M2, K1 etc.), partly to variations in the upstream fetch conditions e.g. the upstream roughness element constituted by summer cottage area in direction 340^o.

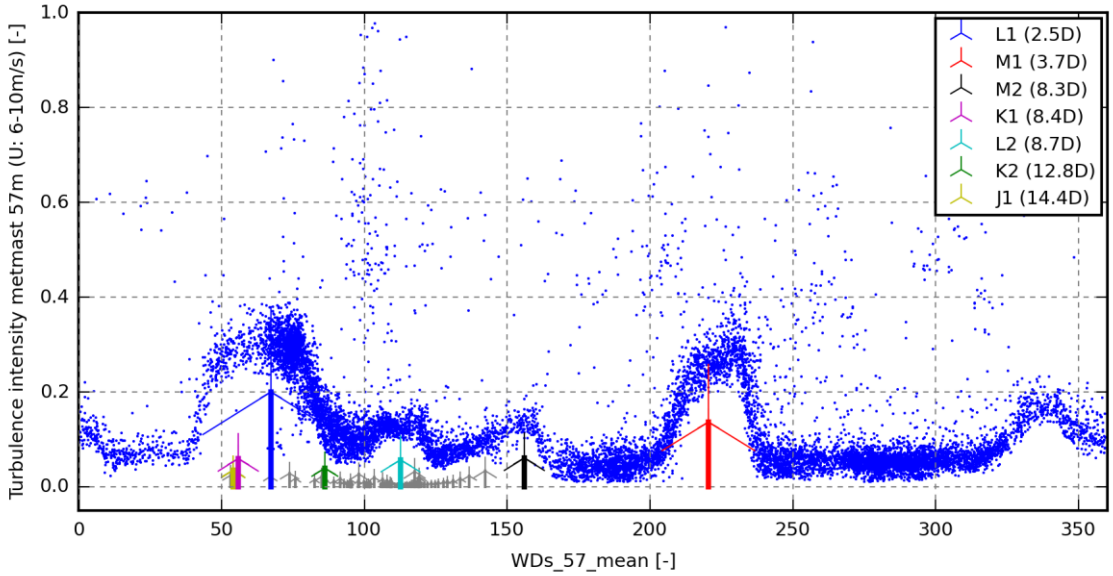

Figure 2. Measured turbulence intensity levels at the Nysted II site.

4. The numerical model

The DWM model complex [3] is based on the combination of three cornerstones: (1) Modeling of quasi-steady wake deficits; (2) a stochastic model of the downwind wake meandering; and (3) added or self-generated wake turbulence, see Figure 3.

The quasi-steady wake deficit is the wake deficit formulated in the moving (i.e. meandering) frame of reference and includes the wake expansion as a function of downstream transportation time caused partly by turbulence diffusion and partly by recovery of the rotor pressure field. The modeling of this deficit is based on a thin shear layer approximation of the Navier–Stokes equations in their rotational symmetric form combined with an eddy viscosity closure. The initial condition is constituted by the induced wind field in the rotor plane determined from a BEM approach. In the present formulation, the aerodynamic module of HAWC2 is used for this purpose. Further details on the implementation can be found in Madsen et al. [4].

The wake meandering part is based on a fundamental presumption stating that the transport of wakes in the atmospheric boundary layer can be modeled by considering the wakes to act as passive tracers driven by the large-scale turbulence structures in lateral and vertical directions [3]. Modeling of the meandering process consequently includes considerations of a suitable description of the 'carrier' stochastic transport media as well as a suitable definition of the cutoff frequency defining large-scale turbulence structures in this context. For the stochastic modeling of wake meandering, we imagine the wake as being constituted by a cascade of wake deficits, each 'emitted' at consecutive time instants in

agreement with the passive tracer analogy [3], [4]. We then subsequently describe the propagation of each of the 'emitted' wake deficits, and the collective description of these thus constitutes the wake meandering model.

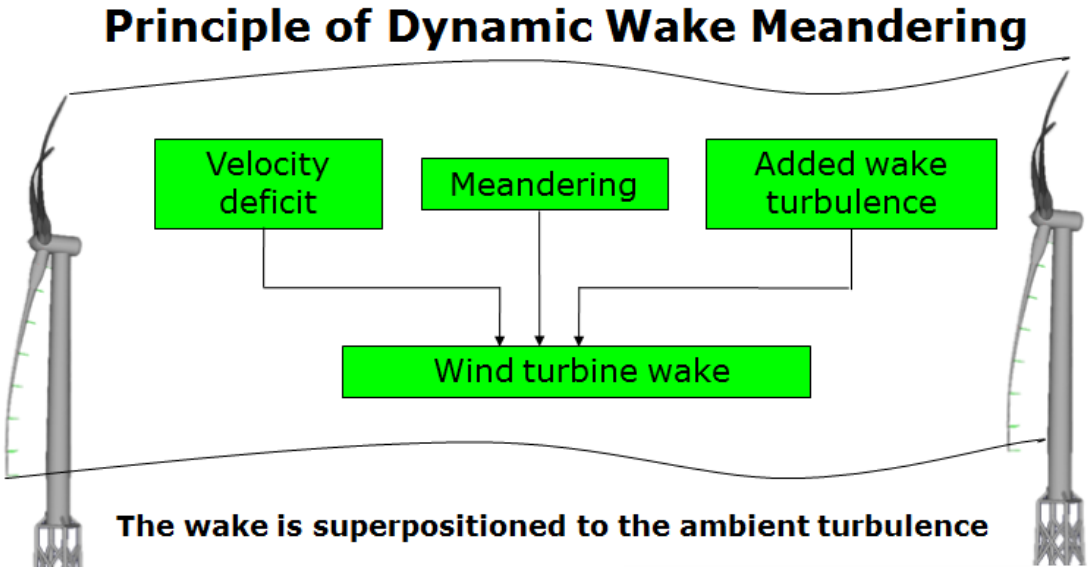

Figure 3. Overview of the three fundamental parts of the DWM model.

Adopting Taylor's hypothesis [7], the downstream advection of these is assumed to be controlled by the mean wind speed of the ambient wind field. With this formulation, the wake momentum in the direction of the mean flow is invariant with respect to downstream displacement. This is a considerable simplification allowing for a straight forward decoupling of the wake along the wind deficit profile (and its expansion) and the wake transportation process. As for the dynamics in the lateral and vertical directions, each considered wake cascade element is displaced according to the large-scale lateral and vertical turbulence velocities at the position of the particular wake cascade element at each time instant. The choice of a suitable stochastic turbulence field, that in turn defines the stochastic wake transport process, is not mandatory, but may be guided by the characteristics of the atmospheric turbulence at the site of relevance. These characteristics encompass in principle not only turbulence standard parameters such as turbulence intensity, turbulence length scale and coherence properties, but also features such as degree of isotropy, homogeneity of the turbulence, Gaussianity of the turbulence, etc.

The DWM model has been implemented into the aeroelastic code HAWC2. This code is based on a multibody formulation as described by Shabana [8] with Timoshenko beam elements as described in [9]. The aerodynamic model is based on an extended BEM model as described in [10]. Validation can be found in [5],[6],[11],[12].

5. Validation:

Measurement are compared to simulations with respect to 1Hz equivalent fatigue loads, see Figure 4-13. Note that all loads are non-dimensionalised with the fatigue load level in the free sector at 9m/s. When comparing the tower bottom bending loads (Figure 4-7) at 8m/s a small offset can be seen in the free sector between the measurement and simulations, however when comparing the relative load level in the wake sectors to the free sector there is an excellent agreement between measurement and simulation. This is yet another indication that the DWM model captures the wake effect very well. The tower yaw loads also have a very fine agreement, which can be seen in Figure 8-9. When comparing loads levels at rated wind speed at 12m/s (Figure 10-11) there is a fine agreement in the multiwake

sector, which is mainly caused by a change in the approach the individual wakes are superimposed, see more about this in [6]. However, the simulated load levels in the single wake situation at 12m/s are significantly underestimated. The reason for this may very well be caused by the simplified way the deficit is evaluated. In the present approach, the deficit is based on the assumption that the upstream turbine operates at the average setting of pitch and rotor speed corresponding to the average ambient wind speed. As the controller has a highly nonlinear influence on the thrust of the turbine, it seems that this leads to slightly underestimated load levels. One solution could simply be to subdivide the results into more narrow wind speed bins, or perhaps to expand the DWM model with a time varying deficit. The latter will be invested in future work.

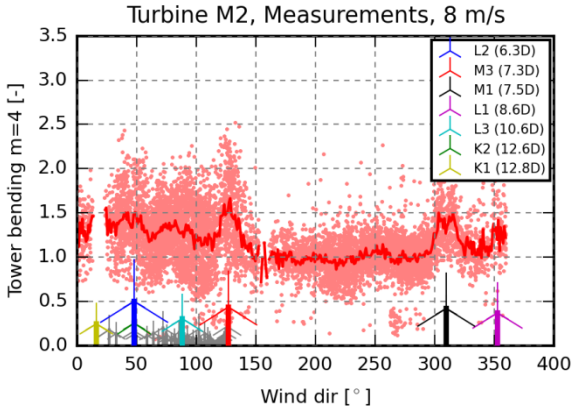

Figure 4. Measured tower bottom bending equivalent moment; WT M2; m = 4; U = 8m/s.

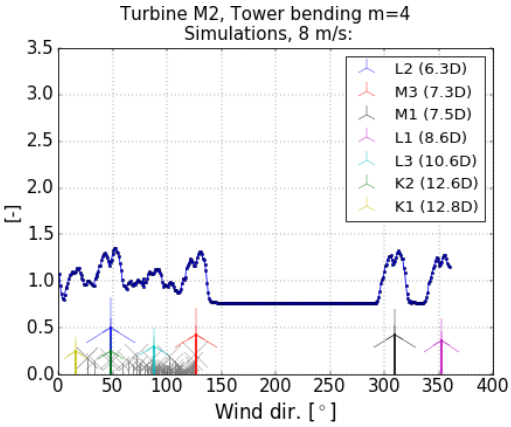

Figure 5. Simulated tower bottom bending equivalent moment; WT M2; m = 4; U = 8m/s.

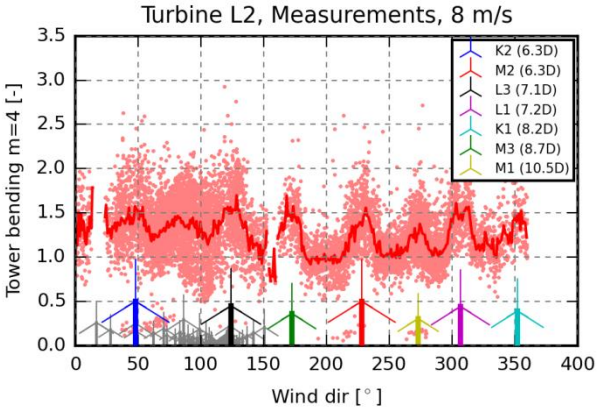

Figure 6. Measured tower bottom bending equivalent moment; WT L2; m = 4; U = 8m/s.

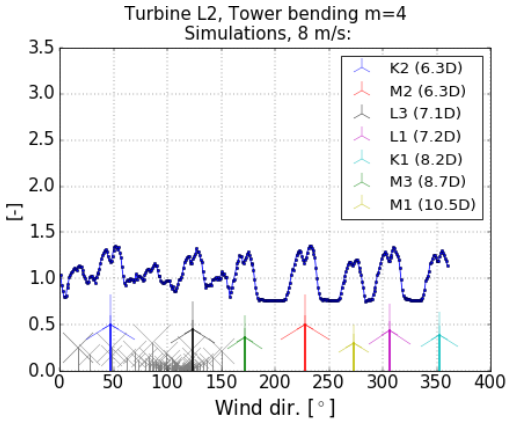

Figure 7. Simulated tower bottom bending equivalent moment; WT L2; m = 4; U = 8m/s.

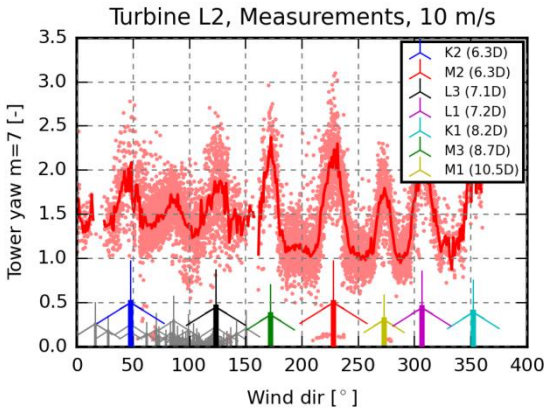

Figure 8. Measured tower top yaw equivalent moment; WT L2; m = 7; U = 10m/s.

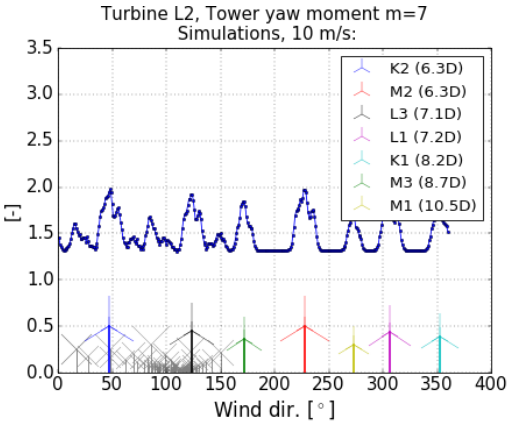

Figure 9. Simulated tower top yaw equivalent moment; WT L2; m = 7; U = 10m/s.

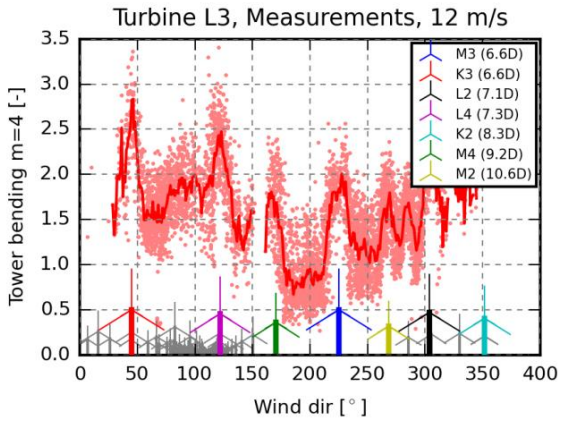

Figure 10. Measured tower bottom bending equivalent moment; WT L3; m = 4; U = 12m/s.

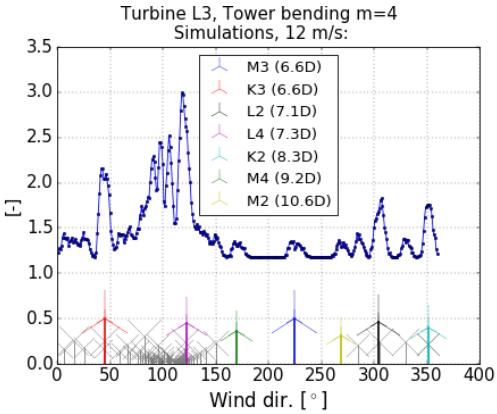

Figure 11. Simulated tower bottom bending equivalent moment; WT L3; m = 4; U = 12m/s.

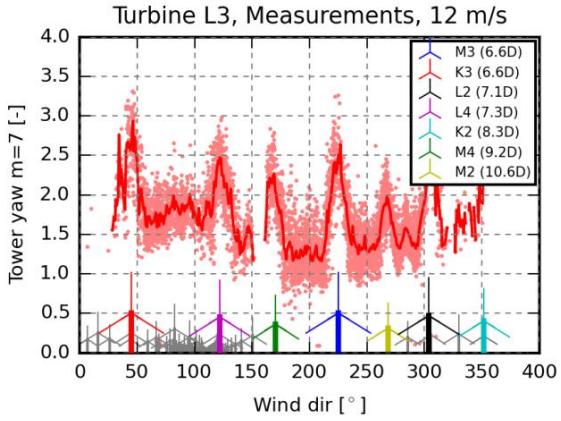

Figure 12. Measured tower top yaw equivalent moment; WT L3; m = 7; U = 12m/s.

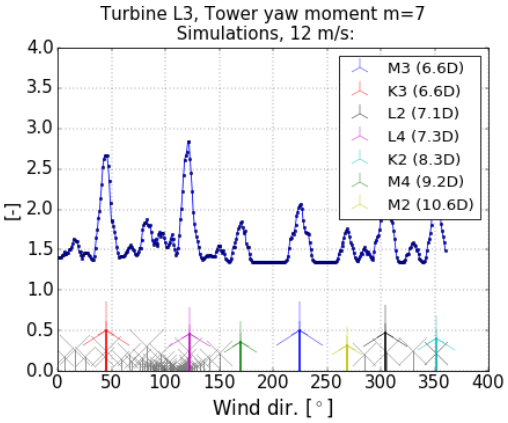

Figure 13. Simulated tower top yaw equivalent moment; WT L3; m = 7; U = 12m/s.

6. Tower loads as function of turbine interspacing

To investigate whether the load levels decrease for increased turbine spacing and find the distance causing the highest load levels, a simulation study was first carried out. It is important to realize that the largest loads may not occur in full wake situations, but in half wake conditions [13]. In Figure 14-16 the load levels of a turbine in a single wake situation were mapped with respect to fatigue load levels as function of wind direction and turbine distance.

At 8m/s the full wake situation shows a rather constant load plateau until 8D spacing for which load decrease beyond this spacing. This, however, only covers a narrow wind direction interval. For wind directions resulting in half wake situations, the loads levels are higher and also continuously decreasing for increased spacing. Therefore, one should expect that for wind speeds below rated, the tower loads are indeed decreasing for increased distance (or the maximum load level is for distances below 4D). This is also seen clearly at 10m/s, Figure 16, where a load peak is identified around 8D for the full wake case. The yaw loads at 8m/s, Figure 15, reveal a distance where the loads have a maximum close to 5D spacing.

Based on the measurements, presented in Figure 17 and 18, it was investigated whether this showed a similar trend. It is not possible from the measurements to identify a certain downstream distance where the loads have a maximum. It is, however, clear to see that between 6.2D until 9D the bending moment loads levels remain on a constant plateau, where a small however clearly visible lower load level is seen for 9-10D spacing's. A similar conclusion can be drawn from the yaw moment measurements. Loads remain at a rather constant plateau until 7D and decrease or further downstream distances.

7. Conclusion

In this study the Nysted II wind turbine park has been analyzed with respect to tower bending load and tower yaw loads. A total of 6 turbines, with different inter spacing's, were fully instrumented with strain gauges. First a load validation between the measured loads and simulated loads using the DWM approach in combination with the aeroelastic code HAWC2 was carried out. A very fine agreement was seen between measurements and simulations in single and multiple wake situations until just below rated wind speed at 12m/s. At 12m/s it seems as the DWM approach under predicts the load levels. It is expected that this is caused by the complex interaction between the nonlinear turbine control characteristics, which may cause a highly varying deficit depth not yet accounted for in the DWM approach.

The measured and simulated cases have also been used to study how load levels vary as function of downstream distance. It is found that the tower bottom bending moments are on same level between 6 and 9D spacing and decreasing for further distances. For the yaw moment, the load levels are on a constant level from 5 to 7D spacing and decreasing for further distances.

8. Acknowledgement

The work was conducted as part of the Energinet.dk project no. 10546 Funded by PSO ForskEL. The writing of the paper has taken place as part of ForskEL under the project Concert (2016-1-12396), which is gratefully acknowledged.

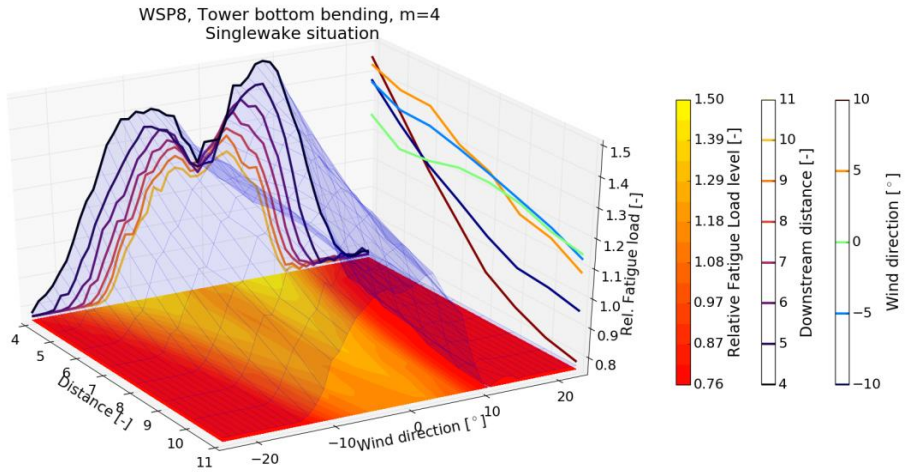

Figure 14. Tower bottom bending moments at 8m/s and 6% turbulence intensity.

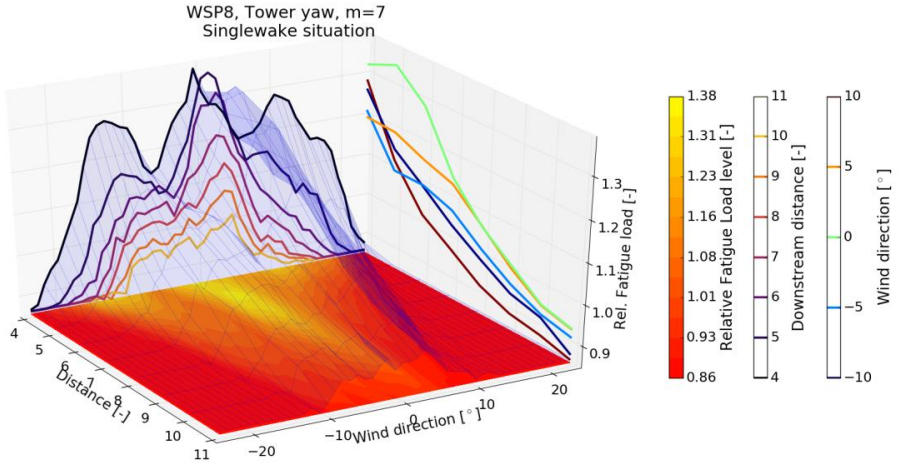

Figure 15: Tower top yaw moments at 8m/s and 6% turbulence intensity.

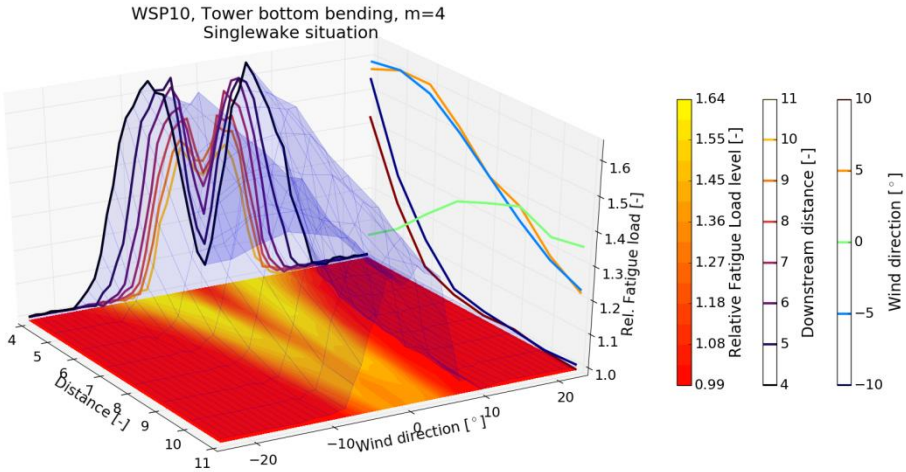

Figure 16: Tower bottom bending equivalent moment; U = 10m/s; TI = 6%.

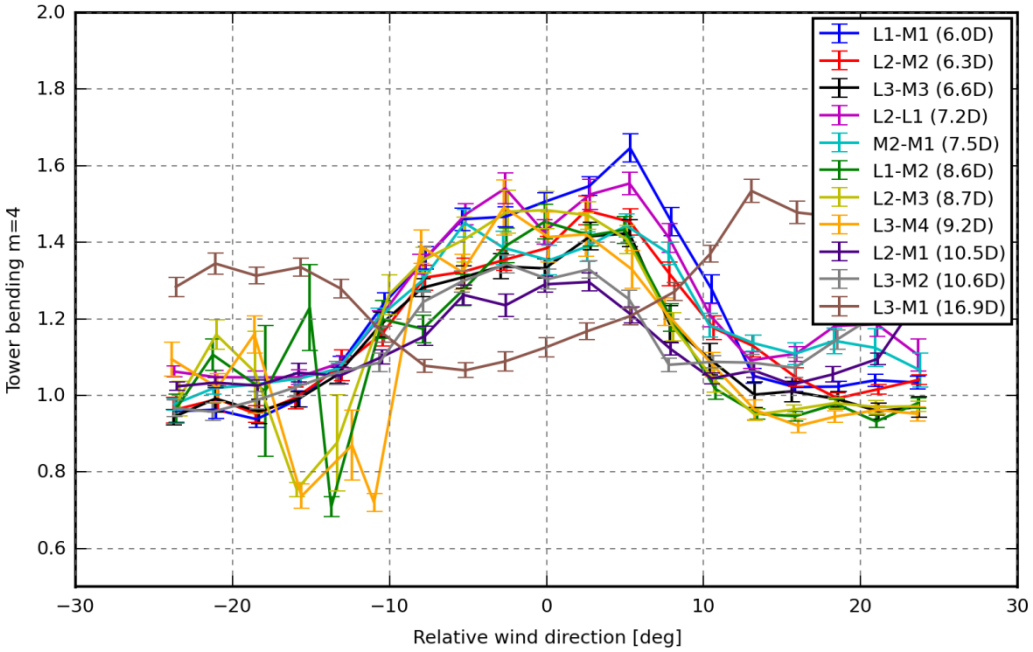

Figure 17: Measured tower bottom bending equivalent moment as function of the relative wind direction between wind and full wake direction; m = 4; U = 8m/s.

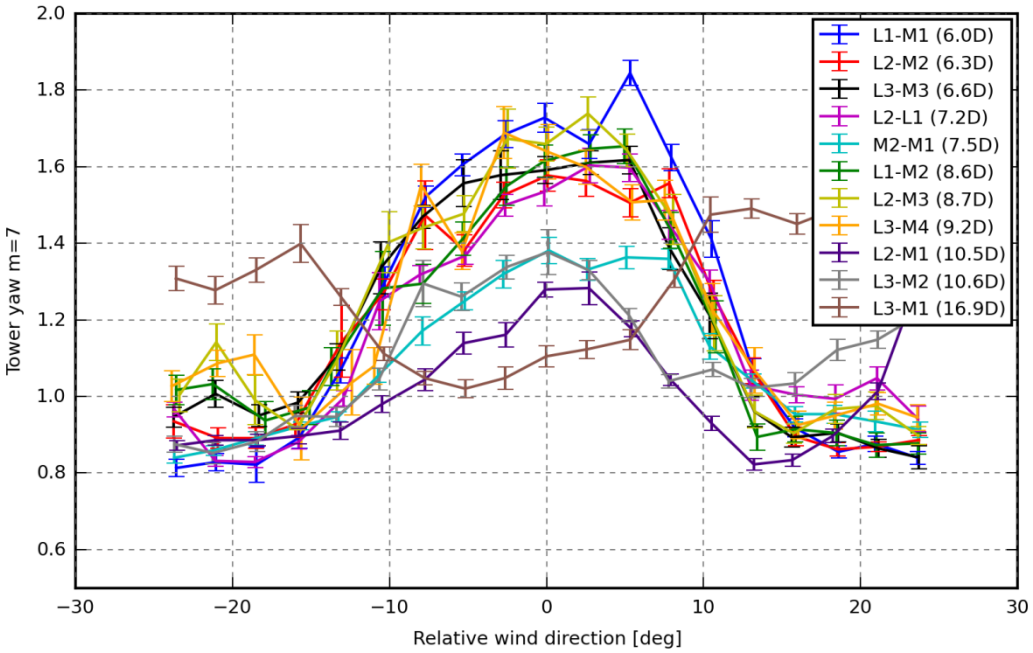

Figure 18: Measured tower top yaw equivalent moment as function of the relative wind direction between wind and full wake direction;
m = 7; U = 8m/s.

References

[1] Frandsen S. Turbulence and turbulence-generated structural loading in wind turbine clusters. Technical Report. Risø-R-1188(EN), Risø-DTU, 2005
[2] IEC 61400-1 ed. 4. Wind turbines - part 1: design requirements.
[3] Larsen, G.C.; Madsen, H.Aa.; Thomsen, K. and Larsen, T.J. (2008). Wake meandering - a pragmatic approach. Wind Energy, 11, pp. 377–395.
[4] Madsen, H.Aa.; Larsen, G.C.; Larsen, T.J.; and Troldborg, N. (2010). Calibration and Validation of the Dynamic Wake Meandering Model for Implementation in an Aeroelastic Code. J. Sol. Energy Eng., 132(4).
[5] Larsen, T.J.; Madsen, H.Aa.; Larsen, G.C. and Hansen, K.S. (2013). Validation of the Dynamic Wake Meander Model for Loads and Power Production in the Egmond aan Zee Wind Farm. Wind Energy, Volume 16, pp. 605–624.
[6] Larsen, T. J., Larsen, G. C., Aagaard Madsen , H., & Petersen, S. M. (2015). Wake effects above rated wind speed. An overlooked contributor to high loads in wind farms. In *Scientific Proceedings. EWEA Annual Conference and Exhibition 2015* (pp. 95-99). European Wind Energy Association (EWEA).
[7] Taylor G. The spectrum of turbulence. Proceedings of the Royal Society London A 1938 1937;164:476-490. DOI:10.1098/rspa.1938.0032
[8] Shabana, A. (1998). *Dynamics of Multibody Systems*. Cambridge University Press: New York.
[9] Kim, T., Hansen, A. M., & Branner, K. (2013). Development of an anisotropic beam finite element for composite wind turbine blades in multibody system. Renewable Energy, 59, 172-183. DOI: 10.1016/j.renene.2013.03.033
[10] Madsen, H.Aa.; Riziotis, V.; Zahle, F.; Hansen, M.; Snel, H.; Grasso. L.T.F.; Politis, E. and Rasmussen, F. (2011). BEM Blade element momentum modeling of inflow with shear in comparison with advanced model results. *Wind Energy*; **15**(1): 63–81.
[11] Vorpahl, F., Strobel, M., Jonkman, J. M., Larsen, T. J., & Passon, P. (2014). Verification of aero-elastic offshore wind turbine design codes under IEA Wind Task XXIII. *Wind Energy*, *17*(4), 519-547. DOI: 10.1002/we.1588
[12] Passon, P., Kühn, M., Butterfield, S., Jonkman, J., Camp, T., & Larsen, T. J. (2007). OC3 - Benchmark exercise of aero-elastic offshore wind turbine codes. *Journal of Physics: Conference Series (Online)*, *75*, 12. DOI: 10.1088/1742-6596/75/1/012071
[13] Steudel, D. Personal communication. 2013.
[14] Hansen, M. H., & Henriksen, L. C. (2013). Basic DTU Wind Energy controller. DTU Wind Energy. (DTU Wind Energy E; No. 0028).